Mechanical Fatigue Behavior under Macroscopically Elastic Stress Cycles Predicted by a Crystal Plasticity FE Analysis†

TSUTSUMI Seiichiro *, YAMATO Naoyuki **, GOTOH Koji *, DUNNE Fionn ******

Abstract

Predicting the mechanical fatigue phenomena of materials subjected to cyclic stresses, the mechanisms on generation and accumulation of inelastic deformation has to be clarified. In this study, a numerical study based on crystal plasticity FE modeling is conducted to evaluate its applicability for the mechanical simulation under uniaxial extension condition through the comparison with the experimental result of a carbon steel (SM400B). Then, the model is applied for the simulation under the symmetrical cyclic loading condition to discuss the effects of inclusions on the fatigue behavior at the stress level lower than the yield stress, i.e macroscopically elastic condition.

KEY WORDS: (polycrystal), (plasticity), (fatigue), (FE analysis), (inclusion)

1. Introduction

Fatigue initiation as a series of damage initiation and accumulation followed by the crack initiation is one of the most challenging issues among the failure processes of materials. Experimental evidence for metals elucidated that the crack initiation is mainly subjected to the damage accumulation which macroscopically/microscopically takes the form of the cyclic plasticity represented by hysteresis loops and ratchetings[1),2)]. To understand and evaluate these fatigue processes of materials, various plasticity models dealing with the mathematical description of the stress–strain relationship have been proposed up to the present [3-7)]. These and extended models are categorized in the framework of unconventional plasticity premising that the interior of the yield surface is not a purely elastic domain[8-12)]. These cyclic plasticity models are originally designed for the mechanical simulation of the loading process under relatively larger stress amplitude than the macroscopic yielding state, which would be categorized in the low- or extremely low-cycle fatigue phenomena.

Not to forget, however, the fact that the fatigue failure of metals could be apparently induced, even if all of the stress amplitudes never exceeded the macroscopic yielding state [13,14)]. Although no clear plastic deformation is observed in the measured stress-strain curve during the initial stage of the fatigue test, plastic strain is gradually generated in concurrence with the increase in the number of cycles, and eventually leads to fatigue crack formation.

On the other hand, the use of the so-called crystal plasticity, micromechanics and the other techniques based on the concept of the homogenization have been progressed recently in understanding the macro- and microscopic mechanical behavior of materials, and their results reinforced the importance of microstructural heterogeneity in local slips for metals [15-21)] and for granular materials[22-25)].

This paper presents the results of crystal plasticity FE analysis on the initiation and accumulation of plastic strain in two-dimensional/random-oriented plane-strain grains with and without the effect of inclusions. The modeling of material is based on a rate-dependent crystal plasticity formulation [18,19),26)] and extended to describe the yield drop phenomenon typically observed in carbon steels, and implemented into commercial FE code using the UMAT user subroutine within ABAQUS implicit. Firstly, the numerical analysis under uniaxial extension condition is carried out, and compared with the experimental stress-strain curve obtained [13,14)] for a carbon steel, SM400B. We then examine the effects of alignment and mechanical properties of inclusions on the deformation behavior represented by the initiation and accumulation of plastic strain during the fatigue process of the assumed material.

† Received on December 26, 2011
* Associate Professor, JWRI, Osaka University
** NIPPON Steel Co. (former student of Kyushu Univ.)
*** Associate Professor, Kyushu University
**** Professor, Oxford University
Transactions of JWRI is published by Joining and Welding Research Institute, Osaka University, Ibaraki, Osaka 567-0047, Japan

2. Crystal plasticity FE modeling

2.1 Crystal plasticity model

The rate-dependent crystal plasticity model [18,19] is implemented into the finite element code ABAQUS implicit. For simplicity, we allow the possibility of the twelve octahedral slip systems to be active in bcc crystals and in the usual way[26], determine the resolved shear stress, τ^{α}, on each system, α, from

$$\tau^{\alpha} = \boldsymbol{\sigma}\boldsymbol{n}^{\alpha} \cdot \boldsymbol{s}^{\alpha} \tag{1}$$

and the plastic velocity gradient is obtained from

$$\boldsymbol{L}^{p} = \sum_{\alpha} \dot{\gamma}^{\alpha} \boldsymbol{s}^{\alpha} \otimes \boldsymbol{n}^{\alpha} \tag{2}$$

where for an active system, for which the critical resolved shear stress is achieved,

$$\dot{\gamma}^{\alpha} = a \sinh b(\tau^{\alpha} - \tau_c - r) \tag{3}$$

else $\dot{\gamma}^{\alpha} = 0$, in which a and b are the rate-sensitivity controlling material parameters. r is introduced to describe hardening/softening of crystal slips, and assumed to be given by a function of

$$r = c[1 - \exp(-d * p)] \tag{4}$$

in which c and d are the hardening/softening controlling material parameters. The magnitude of the accumulated (plastic) slip, p, is defined as

$$p = \int_{t=0}^{T} (\frac{2}{3} \boldsymbol{L}^{p} : \boldsymbol{L}^{p})^{1/2} dt \tag{5}$$

The plastic stretching, $\boldsymbol{D}^{p}$, and spin, $\boldsymbol{W}^{p}$, are determined as the symmetric and anti-symmetric parts of the plastic velocity gradient, respectively, and the slip normals $\boldsymbol{n}$ and directions $\boldsymbol{s}$ are not updated in this study, since the changes can be negligibly small. For the purposes of simplicity, at the crystal level, a hardening/softening function of the form of Equation (4) is introduced. A further assumption made is that of elastic isotropy.

2.2 FE modeling

A crystal plasticity finite element approach has been adopted for the modeling of the uniaxial extension and symmetrical cyclic stressing test, and the two-dimensional model is shown in **Figure 1**. Plane strain analyses have been carried out with 2142 eight node quadrilateral-elements, and forced-displacement is applied on the top surface. However, the intention of the present study is to address grain-level behavior typical of that which occurs in a regular polycrystal under deformation, whilst at the same time, for expediency, retaining simplicity. We therefore consider a model polycrystal comprising 27 grains with the major 12-slip systems in which all the crystallographic orientations and the other conditions (such as material properties and loading conditions) remain unchanged, unless otherwise stated to include effects of elastic inclusions. The polycrystal, with an average grain size of about 20μm, is shown in Fig.1, and all the grains are assigned a crystallographic orientation which is random. The grain

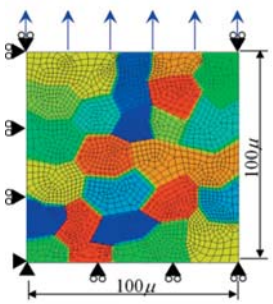

Fig. 1 Analyzed elasto-plastic FE-model O with 27 random oriented crystals and applied boundary condition.

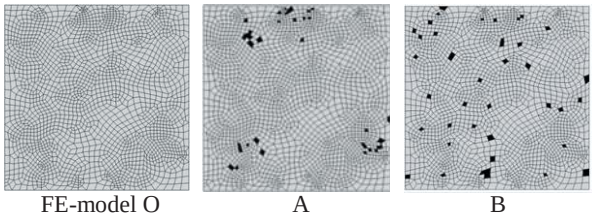

FE-model O (no inclusion) | A (close-set) | B (random)

Fig. 2 Analyzed elasto-plastic FE-model O with 27 random oriented crystals and applied boundary condition.

morphology has been specified arbitrarily to represent that seen in the representative microstructure without imposed texture. In order to assess the importance, or otherwise, of the existence and alignment of softer and/or harder inclusions in the bcc polycrystals, the model under uniaxial and cyclic loading, both with (FE-models A and B) and without (FE-model O, base model) the inclusions are analyzed. The alignments of inclusions are shown in **Figure 2**, in which the inclusions of 1-2 % volume fraction are marked black on the corresponding FE-mesh. Relatively few grains are considered in the model and it should therefore be noted that effect of boundary is likely to be large for grains close to the free surfaces. However, studies on effects of boundary conditions showed limited sensitivity for the macroscopic stress-strain responses under uniaxial loading condition.

As the **Table 1** indicates, the Young's modulus, E, and Poisson's ratio, ν, for the FE-models O, A and B, except for the mesh assigned inclusion, are 206 ($=E_0$) GPa and 0.3 respectively. Also, the critical resolved shear stress of 85 MPa is chosen, and in the present investigation, for the purposes of simplicity, the rate-sensitivity parameters are chosen to give a near-undetectable rate dependence (a = 1.0, b = 0.1), reducing the model, in effect, to one which is rate independent.On the other hand, the mechanical response of the inclusions, marked black on the FE-models A and B, are assumed to be given by the elastic constitutive model of the Young's modulus from $E=E_0/10$ to E_0*10^5, as classified in Table 1.

Table 1 Classification of FE models in terms of property of elastic inclusions.

Material property*	FE-models O, A and B				
E (GPa)	base model (FE-model O)	Elastic inclusions of FE-models A and B			
		a	b	c	d
	206(=E_0)	E_0/10	E_0/2	E_0*2	E_0*10^5

(* Identical for all models: ν=0.3, α=1.0, β=0.1; ** Plasticity parameters: τ_{c0} =85, q=170 and a=10)

Table 2 The chemical composition of SM400B (wt.%).

C	Si	Mn	P	S	Ni	Cr	Mo	C^{eq}
0.15	0.32	1.46	0.014	0.002	0.02	0.03	0.01	0.42

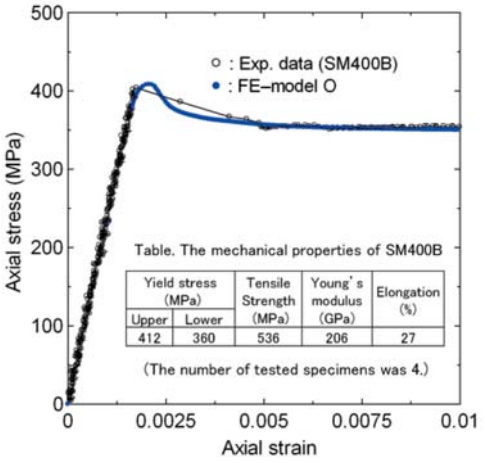

Fig. 3 Experimental stress-strain curve for SM400B together with that predicted by the FE-model O.

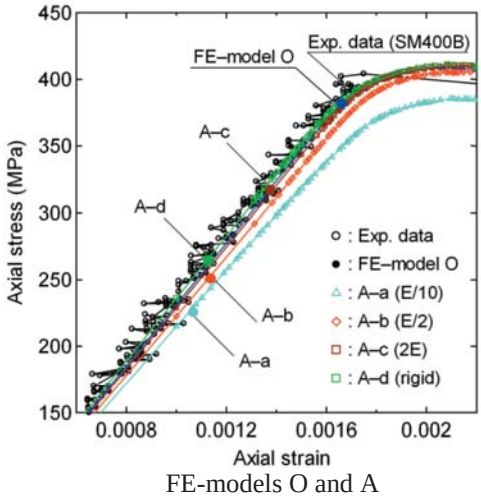

FE-models O and A

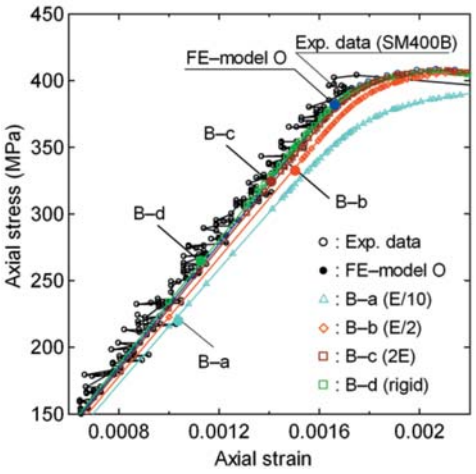

FE-models O and B

Fig. 4 Magnified stress-strain curves around a pre-dominant yield stress predicted by the FE-models O, A and B with experimental result, detecting the points at the first appearance of plastic strain.

3. Comparisons of mechanical responses under uniaxial and cyclic loading conditions

3.1 Experimental results

The material used in the experiment was a typical carbon steel, SM400B, in the shape of round bar, and the experiment was conducted at quasi-static and room temperature conditions [13,14]. The chemical composition of the material is shown in **Table 2**. Strain in the axis direction is measured under uniaxial loading condition by averaging output results of two 2mm strain gages bonded to a specimen. Normal stress-strain plots measured up to axial strain of 0.01 are converted to that of plane strain by using the elasticity assumption as shown in **Figure 3**, together with the results of numerical calculation of the FE-model O, which will be discussed later. As can be seen from the experimental result, the material exhibits upper/lower yielding and plateau behavior with increase of axial strain up to around 0.01. The tensile properties of the material are given in Fig.3.

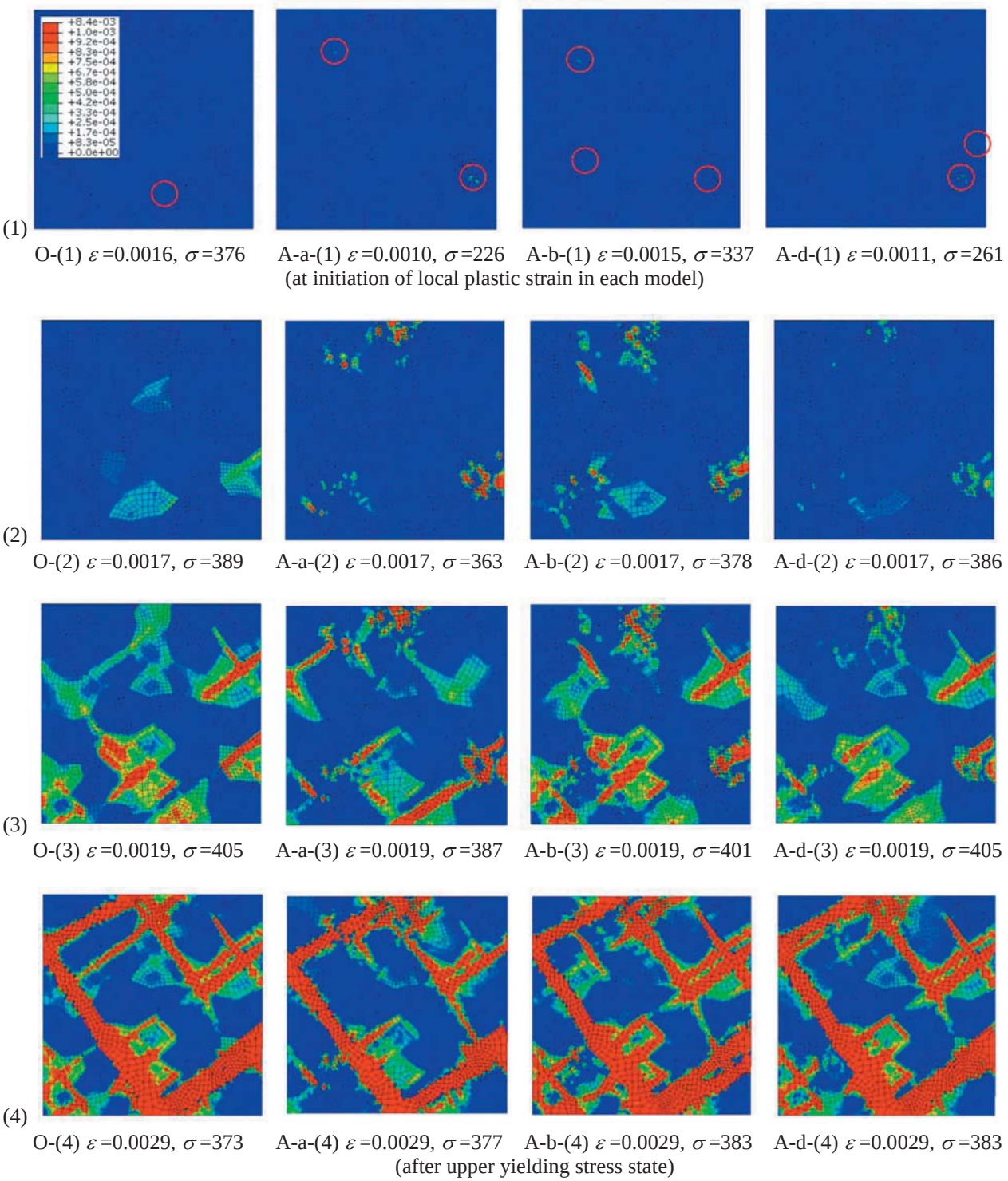

Fig. 5 Distributions of accumulated plastic strain calculated by the FE-models O, A-a, A-b and A-d.

3.2 Numerical results under uniaxial extension condition

Numerical simulations under uniaxial condition were conducted with constant strain rate and the results were compared with the corresponding experimental data in **Figures 3 and 4**. Here, in order to extract the macroscopic behavior, the nodal forces on the top surface of the polycrystal (where the displacement is imposed, as shown in Fig. 1) are summed and divided by the section area. The macroscopic strain in axial direction is also obtained from the change of length of the assembly.

Fig. 4 show the expansion of the stress-strain curves focused on the pre-yield drop regime, and the points for the initiation of plastic strain calculated by the FE-models

are specified on their curves. A yield drop after dominant yielding and a plateau without hardening can be observed experimentally and simulated well irrespective of the existence of elastic inclusions.

Field plots of the accumulated (plastic) slip are shown in **Figure 5** at various stages of deformation ((1)initiation of plasticity, (2) early plastic, (3) around peak stress, and (3) softening regimes) to demonstrate the non-uniform distribution developed because of the ease of achieving multi-slip in the grains. It is demonstrated, therefore, that the model reproduces the expected macro-scale behavior which is representative of the

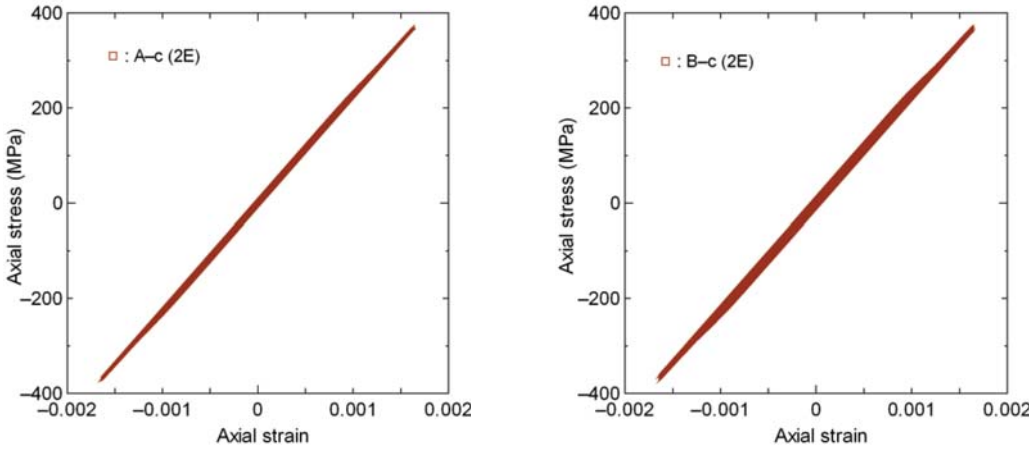

FE-model A-c FE-model B-c

Fig. 6 Stress-strain curve under cyclic loading condition, predicted by the FE-models A-c and B-c.

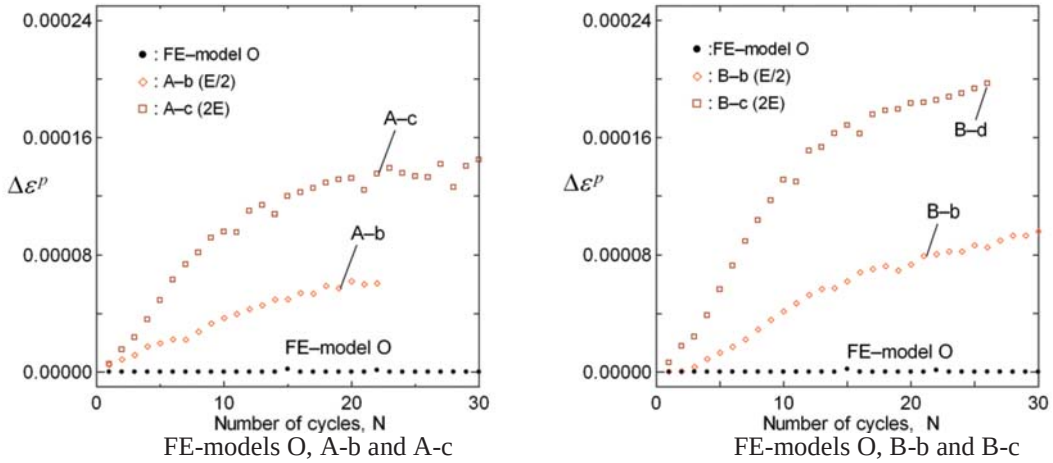

FE-models O, A-b and A-c FE-models O, B-b and B-c

Fig. 7 Evolution of net plastic strain ($\Delta\varepsilon^p$) during the applied loading cycles, predicted by the models O, A and B.

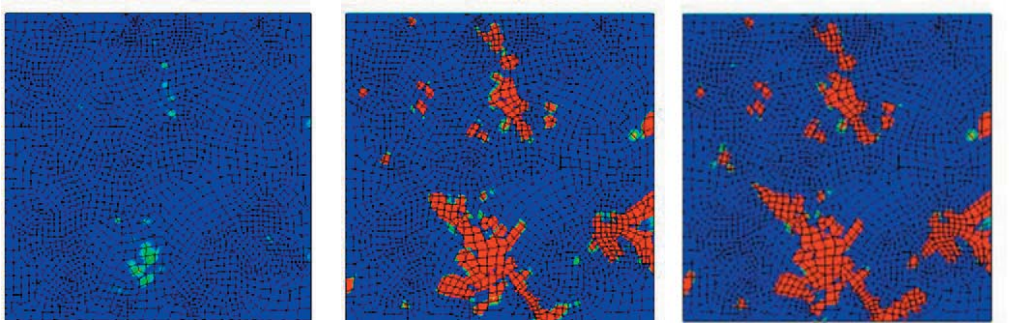

N=1 N=10 N=20

Fig. 8 Evolution of accumulated plastic strain with increase of the applied loading cycles, predicted by the model B-c.

experimental behavior of a carbon steel SM400B. Also, in these figures, considerable decrease of the initiation stress of plastic strain is observed for the models incorporating inclusions than that of FE-model O (no inclusion), and the lowest stresses achieved is predicted by the FE-model A-a and B-a to be around 226 MPa, which is about 60 percent of that predicted by the FE-model O without any inclusion. At the level of macroscopic stress-strain curve, the effect of inclusion on the initiation of local-plastic strain appears to be significant. This is also the case at the grain level, shown in Fig.4. The accumulated slip, *p*, at the first appearance in each model is circled in Fig.5 (1). It shows quite considerable differences of not only the stress (strain) but also of the positions, resulting from the mechanical properties of inclusions. This is also the case at the next level in Fig.5 (2), which shows the results at the same strain level of 0.0017. These analyses show that the initiation of plastic strain is predicted before dominant yielding, while the elastic property of inclusions has a significant effect on the initiation stress of plastic strain in the macroscopically elastic stress state. Here we should remind that the fatigue limit or proportional limit of carbon steels is far lower than the engineering yield stress of the material.

3.3 Numerical results under symmetrical cyclic loading condition

Now, based on the same models adopted previously, numerical simulations of cyclic loading test with symmetrical-displacement controlled condition were conducted for the FE-models O, A-b and B-b. The total number of loading cycles was 30.

In order to understand the phenomenological aspects, the stress-strain curves in axial direction are obtained during fatigue loadings, as shown **Figure 6**. The so-called net plastic strain, $\Delta\varepsilon^p$, extracted at the zero stress level and representing the width of the stress-strain curves, is given in **Figure 7**. Furthermore, the field plots of the accumulated (plastic) slip at the specific number of cycles (N=1, 10 and 20) are demonstrated in **Figure 8**. From these figures, it is demonstrated that the localized accumulated slips calculated during fatigue loadings are expanded in space, and as the results, the stress-strain curve began to expand with increase of accumulated plastic strain. These expansion behaviors of accumulated slip, even during the symmetrical forced-displacement controlled condition, are motivated by the nonlinearity of deformation process trigged by both material nonlinearity and non-homogeneity of deformation, which was enhanced by material softening and heterogeneity of polycrystal. It is also noted, for the boundary condition adopted in this study, that the net plastic strain, $\Delta\varepsilon^p$, was predicted larger for the model adopting harder inclusions as shown in Fig. 6.

3. Concluding

A crystal plasticity FE simulation of uniaxial extension and cyclic loading test conditions have been presented in this study. The analyzed model is based on a crystal plasticity model and extended by incorporating softening function. This model captures several important features of the behavior of a carbon steels under monotonic loading, e.g. upper yielding, yield drop, saturation and early initiation of plastic strain below dominant-yielding stress state. The mechanical responses affected by the existence of elastic inclusions are also discussed. The highlights of this FE analysis results are summarized as follows.

(1) The proposed crystal plasticity model incorporating a softening function describes the yielding behavior of typical carbon steels.
(2) Initiation of plastic strain is predicted below the dominant yielding stress state; that is, macroscopically elastic condition as expected from experimental results on the mechanical fatigue.
(3) The elastic property of inclusions has significant effect on the initiation and accumulation of plastic strain in macroscopically elastic stress state.

The validity of the present model for the simulation of initiation and development of plastic strain should be confirmed by comparing experimental stress-strain responses under monotonic and cyclic loading conditions.

ACKNOWLEDGEMENTS

The support from the Japan Society for the Promotion of Science (JSPS) on Grant-in-Aid for Young Scientists (B)20760562 is greatly appreciated.

REFERENCES

1) Suresh, S.; Fatigue of materials, Cambridge Univ. Press, 1998.Asaro, R.J., Micromechanics of crystals and polycrystals, Adv. Appl. Mech. Vo.23, pp.1-115, 1983.
2) Toyosada, M., Gotoh, K. and Niwa, T.; Fatigue crack propagation for a through thickness crack: a crack propagation law considering cyclic plasticity near the crack tip, Int. J. Fatigue, Vol. 26, pp. 983-992, 2004.
3) Mroz, Z.; On the description of anisotropic workhardening, J. Mech. Phys. Solids, Vol. 15, pp. 163-175, 1967.
4) Dafalias, Y.F. and Popov, E.P.; A model of nonlinearly hardening materials for complex loading, Acta Mech., Vol. 21, pp. 173-192, 1975.
5) Dafalias, Y.F. and Herrmann, L.R.; A bounding surface soil plasticity model, Proc. Int. Symp. Soils under Cyclic Trans. Load., Swansea, pp. 335-345, 1980.
6) Hashiguchi, K.; Subloading surface model in unconventional plasticity, Int. J. Solid Struct., Vol. 25(8), pp. 917-945, 1989.
7) Ohno, N. and Wang, J. -D.; Kinematic hardening rules with critical state of dynamic recovery, part I: formation and basic features for ratcheting behavior, Int. J. Plasticity, Vol. 9(3), pp. 375-390, 1993.
8) Drucker, D.C.; Conventional and unconventional plastic response and representation, Appl. Mech. Rev. (ASME), Vol. 41, pp. 151-167, 1988.
9) Hashiguchi, K. and Tsutsumi, S.; Elastoplastic constitutive equation with tangential stress rate effect, Int. J. Plasticity, Vol. 17(1), pp. 117-145, 2001.
10) Hashiguchi, K. and Tsutsumi, S.; Shear band formation analysis in soils by the subloading surface model with tangential stress rate effect, Int. J. Plasticity, Vol. 19(10), pp. 1651-1677, 2003.

11) Tsutsumi, S. and Hashiguchi, K.; General non-proportional loading behavior of soils, Int. J. Plasticity, Vol. 21(10), pp. 1941-1969, 2005.
12) Hashiguchi, K. and Tsutsumi, S.; Gradient plasticity with the tangential subloading surface model and the prediction of shear band thickness of granular materials, Int. J. Plasticity, Vol. 23(5), pp.767-797, 2007.
13) Tsutsumi, S., Toyosada, M. and Hashiguchi, K.: Extended subloading surface model incorporating elastic boundary concept, J. Appl. Mech. (JSCE), Vol. 9, pp.455-462, 2006.
14) Tsutsumi, S., Murakami, K., Gotoh, K., Toyosada, M.: Cyclic stress-strain relationship during high cycle fatigue process : elastoplastic constitutive model introducing cyclic damage effect, J. of the Japan Society of Naval Architects and Ocean Engineers, Vol.7, pp.243-250, 2008.
15) Manonukul, A., Dunne, F.P.E., Knowles, D., Physically-based model for creep in nickel-bas superalloy C263 both above and below the gamma solvus, Acta Mater., Vol.50, pp.2917-2931, 2002.
16) Bennett, V.P. and McDowell, D.L., Polycrystal orientation distribution effects on microslip in high cycle fatigue. Int. J. Fatigue, Vol.25, pp.27-39, 2003.
17) Osawa, N., Ueno, D., Shimoike, R., Hashimoto, K., Nakashima, K., Nose, T., Numerical study on the fatigue crack propagation behavior in flattened martensite dual phase steel, J. of the Japan Society of Naval Architects and Ocean Engineers, Vol.6, pp.387-397, 2007.
18) Dunne, F.P.E., Wilkinson, A.J., Allen, R., Experimental and computational studies of low cycle fatigue crack nucleation in a polycrystal, Int. J. Plasticity, Vol.23, pp.273-295, 2007.
19) Dunne, F.P.E., Rugg, D., Walker, A., Lengthscale-dependent, elastically anisotropic, physically-based hcp crystal plasticity: Application to cold-dwell fatigue in Ti alloys, Int. J. Plasticity, Vol.23, pp.1061-1083, 2007.
20) Musinski, W.D., McDowell, D.L.; Microstructure-sensitive probabilistic modeling of HCF crack initiation and early crack growth in Ni-base superalloy IN100 notched components, Int. J. Fatigue, Vol. 37, pp. 41-53, 2012.
21) Przybyla, C.P., McDowell, D.L.; Microstructure-sensitive extreme-value probabilities of high-cycle fatigue for surface vs. subsurface crack formation in duplex Ti–6Al–4V, Acta Materialia, Vol. 60 (1), pp. 293-305, 2012.
22) Oda, M.; Inherent and induced anisotropy in plasticity theory of granular soils. Mech. Mater. Vol.16, pp.35–45, 1993.
23) Nicot, F., Darve, F.RNVO Group; A multi-scale approach to granular materials. Mech. Mater. Vol. 37, pp.980–1006, 2005.
24) Kaneko, K., Terada, K., Kyoya, T., Kishino, Y.; Global-local analysis of granular media in quasi-static equilibrium. Int. J. Solids Struct. Vol. 40, pp. 4043–4069, 2003.
25) Tsutsumi, S. and Kaneko, K.; Constitutive response of idealized granular media under the principal stress axes rotation, Int. J. Plasticity, Vol. 24(10), pp. 1967-1989, 2008.
26) Anand, L. and Kothari, M., 1996. A computational procedure for rate-independent crystal plasticity, J. Mech. Phys. Solids, Vol.44, pp.525-558, 1996.